

IMPROVING THE PREDICTIVE POWER OF MODELING THE EMITTER DIFFUSION BY FULLY INCLUDING THE PHOSPHOSILICATE GLASS (PSG) LAYER

H. Wagner¹, A. Dastgheib-Shirazi², R. Chen³, S.T. Dunham³, M. Kessler⁴ and P.P. Altermatt¹

¹Dep. Solar Energy, Inst. Solid-State Physics, Leibniz University of Hannover, Appelstr. 2, 30167 Hannover, Germany

²Div. Photovoltaics, Dep. of Physics, University of Konstanz, 78457 Konstanz, Germany

³Electrical Engineering Department, University of Washington, Seattle WA 98195, USA

⁴Institute for Solar Energy Research Hamelin (ISFH), Am Ohrberg 1, 31860 Emmerthal, Germany

ABSTRACT

Presently, the PV industry is switching to the selective emitter design, where the phosphorus density is significantly reduced between the front metal fingers. Current diffusion models simply adjust the peak phosphorus density at the Si surface to match the measured profiles, and therefore they are unable to predict the necessary gas flows and the temperatures during predeposition and drive-in to realize an optimum emitter profile. In order to achieve better prediction capabilities, we implement a model for the phosphosilicate glass (PSG) layer and for its coupling to silicon. We combine this model with coupled dopant/defect diffusion models in Si to calculate the resulting dopant profiles. With our improvements, we reproduce the profile measurements for a range of POCl_3 flows at temperatures typically chosen in industrial fabrication.

MOTIVATION

The emitter of most crystalline Si solar cells is formed by phosphorus diffusion, and the most common way to achieve this is by forming a phosphorus-rich glass layer, e.g. with a POCl_3 bubbler or a spin-on source. In the selective emitter design, the phosphorus density is significantly reduced between the front metal fingers. The new process conditions are usually found using an empirical approach, e.g. by lowering the temperature in the furnace and by changing the gas flow through the bubbler. The variation of such process parameters can only be done within a rather limited range. For example, lowering the temperature soon results in a diffusion which is too shallow, leading not only to a reduction in phosphorus density, but also to an excessive increase in sheet resistivity. For these and other reasons, the switch to new process parameters to achieve a lower peak dopant density has proven to be rather delicate.

Model calculations promise to accelerate the optimization of the processing conditions. While there are reliable diffusion models for phosphorus, there has been a lack of reliable models for describing the formation of the phosphosilicate glass, and how the glass feeds the phosphorus into the silicon for diffusion. Due to this lack, we are not aware of a model that predicts the phosphorus

profiles reliably as a function of process parameters such as temperature and the flow of gasses. In this paper, we present an improved model and calibrate it on a series of experiments.

FORMATION OF THE PSG LAYER

When Si wafers are exposed to an atmosphere of POCl_3 , O_2 , and N_2 , phosphosilicate glass (PSG) is formed. The glass is a mixture of phosphorus pentoxide (P_2O_5) and silicon dioxide (SiO_2) [1]. This process step is usually called predeposition, and the resulting $\text{P}_2\text{O}_5\text{-SiO}_2$ glass provides a source of phosphorus that diffuses into the Si wafer. Most commonly, an additional process step, called drive-in, follows the predeposition. During drive-in, the supply of reacting gasses is disconnected, and a further amount of phosphorus diffuses into the sample from the existing PSG.

The growth behavior of PSG under ordinary conditions is described as parabolic, with reported thickness values of 10–300 nm [1,2]. Further investigations in Ref. [2] show that for a fixed time and constant flows of reacting gasses, the thickness is also influenced by the process temperature. For example, a 15 min predeposition step at 850 °C gives a thickness value of nearly 27 nm, whereas at 1000 °C a thickness of about 76 nm results. We were unable to find further investigations of the growth behaviour taking also the amount of reacting gasses into account.

A critical process parameter is the concentration of phosphorus in the PSG. This value seems to be affected by the concentrations of POCl_3 and O_2 during predeposition, but a general mathematical expression considering the reacting chemicals does not appear to be available. Depending on the experimental techniques, the reported values for phosphorus concentrations in the PSG are $(2.8 - 4.1) \times 10^{21} \text{ cm}^{-3}$ after low pressure CVD [3] and about $3.8 \times 10^{21} \text{ cm}^{-3}$ after depositing silane and phosphine in an open-tube reactor [4].

EXPERIMENTS

In order to base our model on experimental data, we carried out experiments in which we varied the predeposition time and the POCl_3 flow rates while holding

the temperature constant. The resulting diffusion profile with typical industrial parameters has been analyzed.

In a first set of experiments, the predeposition time was varied among 10 min, 20 min, and 40 min at a fixed temperature of $T = 840^\circ\text{C}$ with constant flows of O_2 and POCl_3 . In this experiment, we used $5 \times 5 \text{ cm}^2$ polished p-type boron-doped float zone (FZ) wafers with a resistivity of $2 \Omega\text{-cm}$. After the RCA cleaning step, the samples were divided into different predeposition groups.

To ensure sufficient comparability among the diffusions, the samples were always placed in the same position in the boat with 75 slots, and surrounded on both sides by 3 clean, undiffused dummies.

After predeposition, the samples were immediately removed from the furnace, hence no drive-in was performed. The resulting phosphorus profiles in silicon were measured with the electrochemical capacitance-voltage technique (ECV) and are shown in Figure 1. As expected, the dose of diffused phosphorus (i.e. the integrated profile) increases with increasing predeposition time, as shown in the inset of Fig. 1.

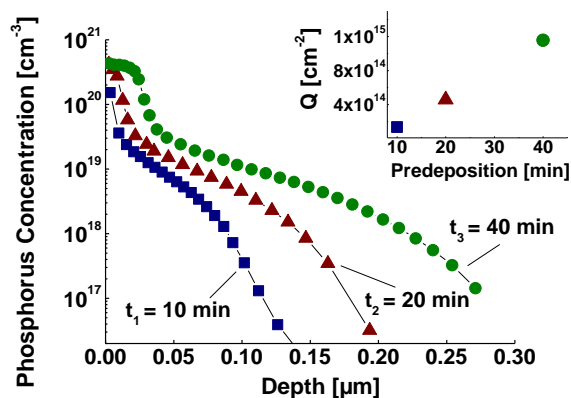


Figure 1 | Phosphorus diffusion profiles in silicon, measured with ECV, obtained with various predeposition times t , while the temperature $T = 840^\circ\text{C}$ and the flows of POCl_3 and O_2 were kept constant. The inset shows the dose of phosphorus (Q) that entered the silicon, calculated by integration over the ECV profile.

In a subsequent experiment, the predeposition time and temperature were kept constant at $t = 10 \text{ min}$ and $T = 840^\circ\text{C}$, respectively, while the flow of POCl_3 was varied from A = 250 sccm to B = 500 sccm and C = 1000 sccm with a constant flow of O_2 . The resulting ECV profiles in silicon are shown in Fig. 2.

This experiment confirms that the dose Q in silicon increases with increasing POCl_3 flow, as shown in the inset, and may be explained by a higher concentration of phosphorus in the PSG layer. According with Fick's law, a higher concentration of P in the PSG layer leads to a stronger gradient of the phosphorus density towards the silicon and therefore to a higher amount of diffusing species.

Figure 3 shows the ECV profiles of the same samples with an additional drive-in process of 10 min. The inset shows the dose of diffused phosphorus, calculated by integration over the profile and by subtracting the amount of Fig. 2 that already diffused during the predeposition. In all three cases, nearly the same amount of phosphorus entered the silicon during predeposition as during the drive-in. Since both the predeposition as well as the drive-in lasted for 10 minutes, the experiment confirms that the PSG layer acts as a rather constant dopant source in this time frame.

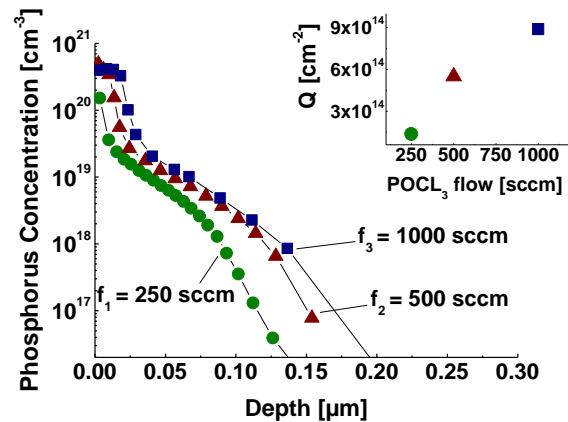


Figure 2 | Phosphorus diffusion profiles in silicon, measured with ECV, obtained with various POCl_3 flows, while the temperature (840°C) and the predeposition time (10 min) were kept constant. The inset shows the dose of phosphorus (Q) that entered the silicon, calculated by integration over the ECV profile.

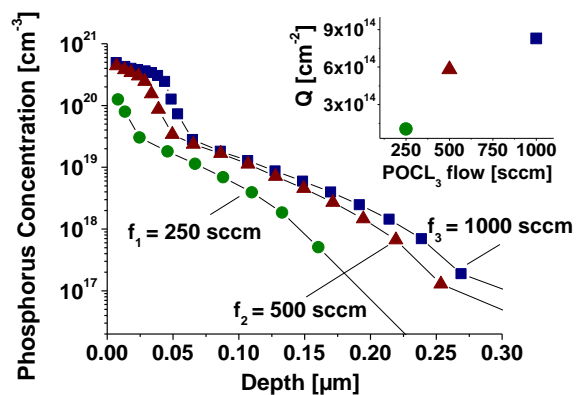


Figure 3 | Phosphorus diffusion profiles as in Fig. 2, processed with an additional drive-in of 10 minutes for each sample. The inset shows the dose of phosphorus (Q) that entered the silicon during the drive-in, calculated by integration over the ECV profile and by subtracting the amount already diffused during the predeposition in Fig. 2.

In a further experiment shown in Fig. 4, 20 min of predeposition and 20 min of drive-in at $T = 845 \text{ }^\circ\text{C}$ was carried out to create a source as typically applied in industry. This time, the profiles were measured with both the ECV technique and secondary ion mass spectroscopy (SIMS). The ECV technique provides the density of substitutional phosphorus, while the SIMS measurements yield the atomic density of phosphorus. At high dopant densities, the two values differ because part of the phosphorus atoms does not occupy substitutional lattice sites and thus is electrically inactive [5]. At large depth, the two profiles differ as well. In SIMS, the phosphorus density may be overestimated due to ion mixing, segregation and surface roughness associated with the relatively high-energy (14.5 keV) Cs^+ ion beam. In ECV, carrier spilling effects associated with the pn-junction depletion region may lead to an underestimation of the phosphorus density by 30 nm (or 100 nm) at phosphorus densities below 10^{17} cm^{-3} (or 10^{16} cm^{-3}) [6].

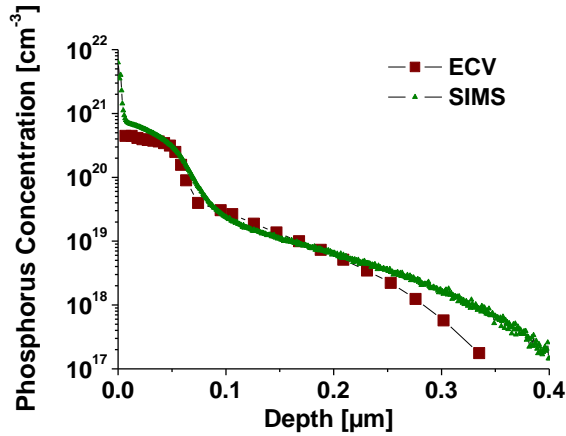


Figure 4 | Phosphorus diffusion profile after 20 min of predeposition and 20 min of drive-in at $T = 845 \text{ }^\circ\text{C}$, measured with ECV and SIMS.

All these results confirm that the diffusion profile in silicon is highly affected by the conditions under which a PSG is formed. Basic conditions like time and temperature for predeposition and drive-in have to be considered, and the reacting chemicals during predeposition also play an important role.

SIMULATION

In this section, we improve the model to numerically reproduce the experiments described above. We describe the phosphorus diffusion in silicon with the pair-diffusion model of Refs. [7,8], where phosphorus diffuses via pairing with interstitials (I) and vacancies (V). Fermi level dependencies of various charge states are taken into account to capture the kink and tail of the diffusion profile. Here, we focus on the PSG layer and its interface to silicon.

Within the PSG layer, we assume that phosphorus diffuses according to the linear diffusion equation:

$$\frac{\partial C_{PSG}}{\partial t} = D_{PSG} \frac{\partial^2 C_{PSG}}{\partial x^2} \quad (1)$$

where $C_{PSG} [\text{cm}^{-3}]$ is the concentration of phosphorus and $D_{PSG} [\text{cm}^2/\text{s}]$ the diffusivity. The diffusivity D_{PSG} of phosphorus in the PSG layer is assumed to have Arrhenius behaviour [9],

$$D_{PSG} = a \cdot \exp\left(-\frac{b eV}{k_B T}\right) \quad (2)$$

where a is the pre-exponential factor, b the activation energy, k_B is the Boltzmann constant and T the absolute temperature.

To model the flux of phosphorus through the PSG silicon interface, we implement a segregation boundary condition, where the flux depends on the phosphorus concentration on the PSG side of the interface, C_{PSG} , and the silicon side, C_{Si} , using the following relationship:

$$J = k_{seg} \left(C_{PSG} - \frac{C_{Si}}{r} \right) \quad (3)$$

The parameter k_{seg} is the diffusion-limited transfer rate, which has a dimension of velocity $[\text{cm}/\text{s}]$ and is determined by

$$k_{seg} = \frac{D}{L} \quad (4)$$

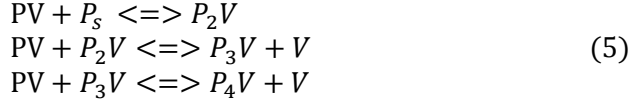
where L is the atomic hopping distance of the diffusion process, usually in the order of several angstroms. We choose k_{seg} rather large ($> 10^{-8} \text{ cm}/\text{s}$) so that equilibrium of the phosphorus concentration on both sides of the interface is established quickly. This implies that diffusion through the interface is fast enough so that the choice of k_{seg} has little influence on the diffusion profile in silicon. The parameter r is the segregation coefficient of phosphorus between the PSG layer and silicon.

As boundary condition at the interface between the PSG layer and the surrounding gas we choose zero flux, because there is no direct evidence of significant outdiffusion to the surrounding gas, and the simulation results are not sensitive to this parameter.

We would like to calibrate the model with the experiments of the previous section. Hence, we also need to quantify the ratio between the amount of active dopants and of the atomic phosphorus density in silicon. The difference of the SIMS and ECV profiles near the interface region suggests that a certain amount of phosphorus atoms forms aggregates that are not electrically active. Here we introduce a phosphorus-vacancy clustering model to

capture this behaviour. In this model, each vacancy binds with up to 4 phosphorus atoms, forming P_nV ($n=2,3,4$) clusters which are neither mobile nor electrically active.

These dopant-vacancy clusters are considered as the dominant species in the deactivation kinetics of arsenic [11, 12]. Here we assume that P_nV clusters are also dominant in the deactivation of phosphorus. The clustering reactions are:



where P_s is a substitutional electrically active phosphorus. The reaction terms of these are determined as:

$$R_1 = k_1 \left(C_{PV} C_{P_s} - \frac{C_{P_2V}}{h_1} \right) \quad (6)$$

$$R_2 = k_2 \left(C_{PV} C_{P_2V} - \frac{C_{P_3V} C_V}{h_2} \right) \quad (7)$$

$$R_3 = k_3 \left(C_{PV} C_{P_3V} - \frac{C_{P_4V} C_V}{h_3} \right) \quad (8)$$

where the k_i 's ($i=1,2,3$) are the kinetic rate factors [cm^3/s] and the h_i 's ($i=1,2,3$) are the equilibrium constants with h_1 in units of [cm^{-3}] and h_2, h_3 are dimensionless. Assuming the reactions are all diffusion limited, we have

$$k_i = 4\pi a^2 \frac{D}{L} \quad (9)$$

where a is the capture radius, D is the diffusivity, and L is the atomic hopping distance of the mobile reacting species (PV). Note that this equation differs from Eq. (4) because of the different geometry (3D vs. 1D).

The h_i 's determine the number of clusters formed for the given dopant and vacancy concentrations and will be used as fitting parameters to match the SIMS and ECV profiles in the interface region.

In the SIMS profiles of Fig. 4, a pile-up of phosphorus is evident near the PSG-silicon interface. These we will model with interface trap sites. Mobile phosphorus species (phosphorus point defect pairs) segregate into the interface traps and release free point defects via:



where T_e is an empty trap site that is not filled by phosphorus, and P_T is a trapped phosphorus, which is neither mobile nor electrically active. The forward rate is proportional to the number of empty trap sites in the trap region, while the reverse rate is proportional to the number of filled trap sites.

For this procedure the diffusion equations for silicon from Ref. [7, 8] and for the PSG Eq. (1) are solved for each time step. At the segregation boundary, the last value at the right site in PSG (cf. below) and the first value at the left site in silicon (initially 0) are used to determine the flux in Eq. (3). After one time step the concentration values at the analyzed nodes close to the boundary are updated according to the flux. Basically, the amount of P that is lost in the PSG region now enters the silicon and is used for solving the differential equations regarding to Ref. [7, 8], the cluster model and the trap sites.

We calibrated this model with our experimental data for different predeposition times and are able to numerically reproduce all the profiles shown in Figs. 5, 6 and 8 with a consistent set of parameters. The kinetic rate factors are $k_i=2.72 \times 10^{-13}$ [cm^3/s] for $i=1,2,3$ at 840 °C and $k_i=3.01 \times 10^{-13}$ [cm^3/s] for $i=1,2,3$ at 845 °C, respectively. The equilibrium constants are $h_1=1.073 \times 10^{20}$ [cm^{-3}], $h_2=h_3=6.14 \times 10^{-3}$ at 840 °C and $h_1=1.14 \times 10^{20}$ [cm^{-3}], $h_2=h_3=6.58 \times 10^{-3}$ at 845 °C.

We find that the P profiles in the Si depend on $C_{PSG}/(D_{PSG})^{1/2}$. It was reported earlier [9] that phosphorus diffusion within the PSG layer is enhanced compared to pure SiO_2 , and that the phosphorus diffusivity increases with increasing concentration of phosphorus in the PSG. They reported that at concentrations of about $3 \times 10^{21} \text{ cm}^{-3}$ the values they report already underestimate observed diffusion. In our study, the diffusivity D of phosphorus used in the PSG layer is 3.89×10^{-16} [cm^2/s] at 840 °C and 4.21×10^{-16} [cm^2/s] at 845 °C. These values are about one order of magnitude higher than reported in Ref. [9]. The diffusivity was chosen to give concentrations of phosphorus in the PSG of $(3.2 - 6.0) \times 10^{21} \text{ cm}^{-3}$, in the range reported in other PSG producing techniques [3, 4].

The interface trap sites have an assumed surface density of $1.4 \times 10^{15} \text{ cm}^{-2}$ equal to the planar silicon lattice density [13]. Due to our choice of parameters it turned out that around 90% percent of the trap sites are filled by phosphorus, corresponding to a dose loss on the order of 10^{15} cm^{-2} due to interface segregation.

The thickness d_{PSG} of the PSG layer is modelled by analysing the growth rates consistent with Ref. [2]. The resulting equation is

$$d_{PSG} = c \cdot \sqrt{t} \quad (11)$$

where $c = 6.40 \pm 0.04$ [$\text{nm}/\text{min}^{1/2}$] is a fitting parameter and t [min] is the predeposition time. This equation does not take the influence from different flow rates on d into account. Due to this simplification, we did further simulations by changing the thickness within a realistic range, and found no influence on our simulated profiles. Thus, Eq. (11) was further used for thickness calculations for $T=840$ °C and $T=845$ °C.

The parameter r in Eq. (3) is the segregation coefficient of phosphorus between the PSG layer and silicon. We choose the same value as for pure SiO_2 , which is approximately 10 [10]. Again, as k_{seg} is high, the value of r has little influence on the phosphorus profile in silicon.

Fig. 5 compares the modeling results (lines) to the experiment (symbols). Plotted are the simulated total P profiles in the PSG and the substitutional P in the silicon in order to compare it to the ECV measurements (where only the amount of electrical active phosphorus is detected). The simulations show a kink and tail behavior comparable to the experimental results.

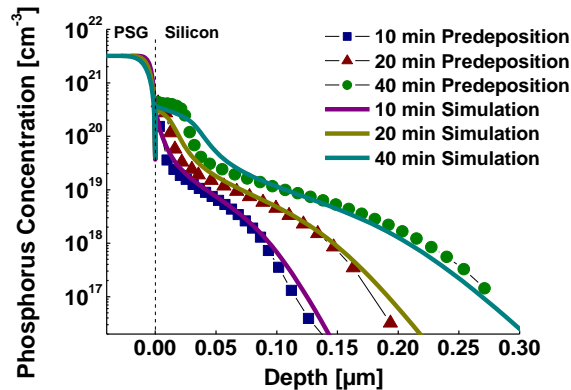


Figure 5 | Simulation (lines) of the experimental phosphorus profiles (symbols) shown in Fig. 1, in dependence of the predeposition time. In the PSG layer, the total P density is plotted, while in Si only the density of active dopants (to make it comparable to the ECV measurement).

As shown in the previous section, approximately the same amount of phosphorus diffuses into silicon during 10 min of predeposition as during 10 min of drive-in. Fig. 6 shows both the predeposition and drive-in. Again, only the electrical active amount of diffused phosphorus is shown. The simulated results match the experimental values within a range of acceptance.

Fig. 7 shows the dose Q of active P in Si calculated with our calibrated model versus time (upper plot) or the phosphorus density in the PSG layer (lower plot) under the same conditions as in Figs. 1 to 3 (i.e. $T = 840\text{ }^{\circ}\text{C}$ and a concentration of $3.2 \times 10^{21}\text{ cm}^{-3}$, or a concentration of P in the PSG in the range of $(0.7-9.2) \times 10^{21}\text{ cm}^{-3}$ with a constant time of 20 min. Both profiles show a nonlinear behavior. The time variation (Fig. 7 upper plot) can be matched approximately with a parabolic increase and closely matches the experimental observations. The variation with concentration of P in PSG (Fig. 7 lower plot) shows a much more nonlinear behavior. There appears to be a minimum concentration ($1.5 \times 10^{21}\text{ cm}^{-3}$) before there is significant incorporation of P in Si and then Q seems to be saturating at high concentrations. The low C behavior can be attributed to segregation to interface traps which eventually get mostly filled, allowing P to diffuse into Si. The lower slope at higher C is due to the formation of inactive P_nV complexes within the model.

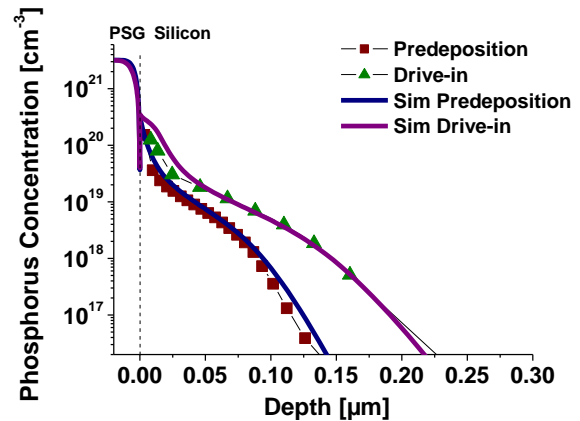


Figure 6 | Simulation (lines) of the experimental phosphorus profiles (symbols) shown in Fig. 2 and 3 for a POCl_3 flow of 250 sccm during predeposition. The time for predeposition and drive-in was 10 min, respectively. In the PSG layer, the total P density is plotted, while in Si only the density of active dopants (to make it comparable to the ECV measurement).

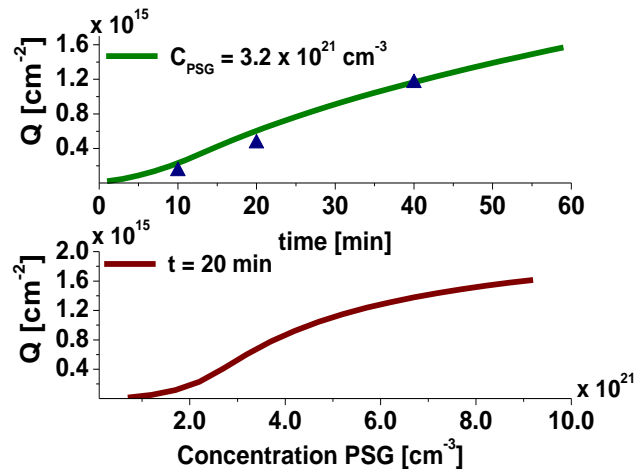


Figure 7 | Calculated dose of phosphorus (Q) diffused into silicon versus time (top) or phosphorus concentration in the PSG layer (bottom) at $T = 840\text{ }^{\circ}\text{C}$. Blue triangles correspond to experimental data in Fig. 1.

Finally, the experiment shown in Figure 4 is simulated and presented in Figs. 8, 9. Plotted are the total P concentration in the PSG layer, the electrically active amount of phosphorus in the silicon (for comparison with the ECV measurements) as well as the total P concentration from the cluster model (for comparison with SIMS data) and the trap sites (for comparison with pile-up of phosphorus near the PSG-silicon interface). Fig. 9 shows a detail of the interface between PSG and silicon from the same results. Good agreement with both profiles is obtained. Note that both simulation curves merge at the

end of the plateau as can also be seen in the experimental ECV and SIMS data.

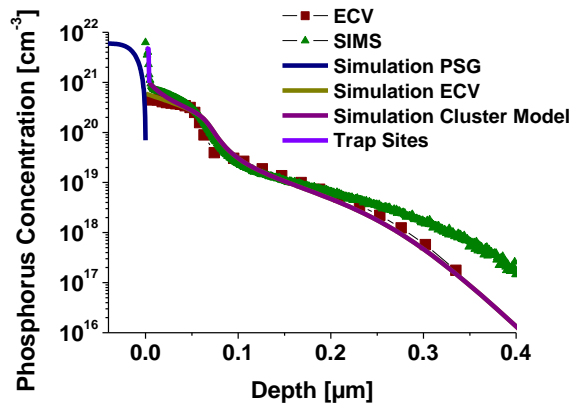


Figure 8 | Simulation (lines) of the ECV profile (electrically active phosphorus) and the SIMS profile (total phosphorus) as compared to the experimental data (symbols) shown in Fig. 4.

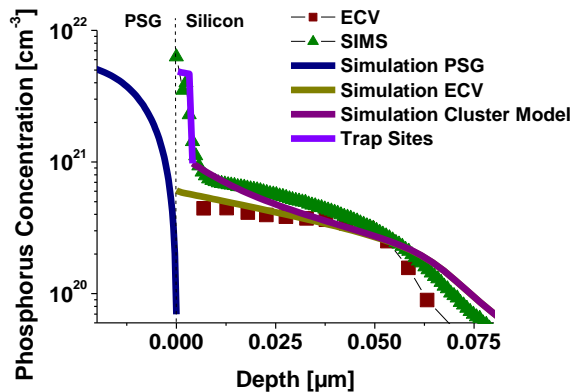


Figure 9 | Detail from Fig. 8 in the interface region.

OUTLOOK

We have shown experimental and simulated results for different times and POCl_3 flows. Our model matches these data for experimental ECV and SIMS profiles. In future work, we would like to present further results over different temperatures and will include an improved model for the formation of the phosphosilicate layer.

REFERENCES

[1] J. Dathe, W. Müller, and L. Grasser, "Wachstum und Eigenschaften von Phosphorgläsern auf Siliziumoberflächen," *Z. angew. Physik* **30**, 1970, pp. 272-275.
 [2] P. Negrini, D. Nobili, and S. Solmi, "Kinetics of Phosphorus Predeposition in Silicon Using POCl_3 ," *J. Electrochem. Soc.* **122**, 1975, pp. 1254-1260.

[3] R. A. Levy, S. M. Vincent, and T. E. McGahan, "Evaluation of the Phosphorus Concentration and Its Effect on Viscous Flow and Reflow in Phosphosilicate Glass," *J. Electrochem. Soc.* **132**, 1985, pp. 1472-1480.
 [4] M. L. Polignano, P. Picco, and G. F. Cerofolini, "Phosphorus Silica Glass as Dopant Source," *J. Electrochem. Soc.* **127**, 1980, pp. 2735-2738.
 [5] S. Solmi, A. Parisini, R. Angelucci, and A. Armigliato, "Dopant and Carrier Concentration in Si in Equilibrium with Monoclinic SiP Precipitates," *Phys. Rev. B* **53**, 1996, pp. 7836-7841.
 [6] Private communications with Thomas Wolff, Ingenieurbüro WEP, Furtwangen (Germany).
 [7] S. T. Dunham, "A Quantitative Model for the Coupled Diffusion of Phosphorus and Point Defects in Silicon," *J. Electrochem. Soc.* **139**, 1992, pp. 2628-2636.
 [8] H. Bracht, "Self- and Foreign-Atom Diffusion in Semiconductor Isotope Heterostructures.II. Experimental Results for Silicon," *Phys. Rev. B* **75**, 2007, pp. 035211 (1-15).
 [9] G. F. Cerofolini, M. L. Polignano, and P. Picco, "Phosphorus Diffusion into Silicon from Chemically Vapour-Deposited Phosphosilicate Glass," *Thin Solid Films* **87**, 1982, pp. 373-378.
 [10] J. D. Plummer, M. Deal, and P. B. Griffin, "Silicon VLSI Technology: Fundamentals, Practice and Modeling," Upper Saddle River, NJ: Prentice Hall, 2000.
 [11] C. Ahn and S. T. Dunham, "Charge Carrier Induced Lattice Strain and Stress Effects on As," *Appl. Phys. Lett.* **93**, 2008, pp. 022112 (1-3).
 [12] M. A. Berding, A. Sher, M. van Schilfgarde, P. M. Rousseau, and W. E. Spicer, "Deactivation in Heavily Arsenic-Doped Silicon," *Appl. Phys. Lett.* **72**, 1998, pp. 1492-1494.
 [13] R. S. Muller, T. I. Kamins, and M. Chan. "Device Electronics for Integrated Circuits." New York, NY: John Wiley & Sons, 2003.